

AD-A056 413

ARMY ELECTRONICS RESEARCH AND DEVELOPMENT COMMAND WS--ETC F/G 20/5
IN SITU MEASUREMENTS OF AEROSOL ABSORPTION WITH A RESONANT CW L--ETC(U)
JUN 78 C W BRUCE, R G PINNICK, R J BREWER

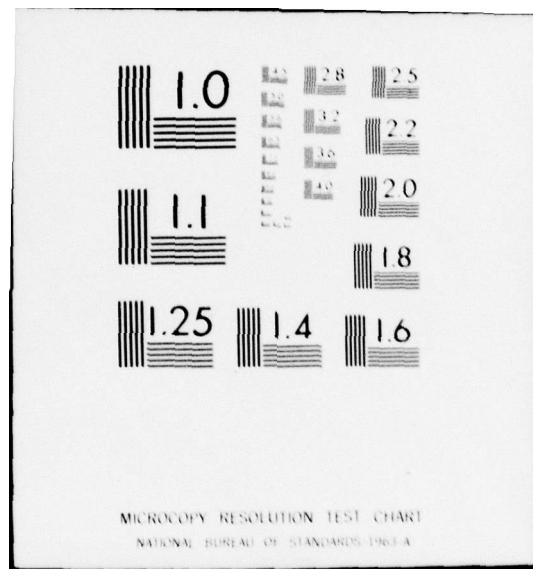
UNCLASSIFIED

NL

1 OF 1
AD
A056 413



END
DATE
FILMED
8 -78
DDC



LEVEL II

AD A 056413

*BRUCE, PINNICK, BREWER, YEE, and FERNANDEZ

⑥ IN SITU MEASUREMENTS OF AEROSOL ABSORPTION
WITH A RESONANT CW LASER SPECTROPHONE

⑪ JUN 1978

⑩ CHARLES W. BRUCE, DR.
RONALD G. PINNICK, DR.
RALPH J. BREWER, DR.
YOUNG P. YEE, DR.
GILBERT FERNANDEZ, DR.

US ARMY ATMOSPHERIC SCIENCES LABORATORY
WHITE SANDS MISSILE RANGE, NM 88002

⑫ 15P

DDC
RECEIVED
JUL 10 1978
D

A major problem area for DOD electro-optical (EO) systems, from concept to operation, is the transmission losses due to atmospheric gaseous and particulate constituents. Atmospheric effects on high energy lasers are usually considered separately from those affecting other EO systems such as target ranging, laser guidance, target designation, forward looking infrared, etc. This is because high energy lasers interact with the atmospheric medium dynamically, changing its nature, while the performance of the remaining EO systems is determined linearly from measurements of the components of the losses, i.e., absorption, scattering, and refractive effects. However, measurements of these quantities plus additional information such as values of meteorological parameters and identification by absorbing constituents form the basis for nonlinear predictions of the transmission of high energy laser energy as well.

In this paper we discuss in situ measurements of the absorption of infrared radiation primarily by atmospheric particulate matter. Absorption itself is of prime importance in determining the high energy laser beam transmission losses, while for the EO systems it is simply additive with the scattering and refractive losses.

Absorption by particulates is currently a major concern in both of the previously mentioned types of systems because this quantity is highly variable with the meteorological and battlefield

DISTRIBUTION STATEMENT A

Approved for public release;
Distribution Unlimited

410 663 78 06 12 057

508

AD Nu.

DDC FILE COPY

conditions and has not been well identified in either composition or magnitude. It is known that particulate absorption can be orders of magnitude below the gaseous absorption. For example, this is typical for the 10 μ m "transmission window" in a quiescent atmosphere. However, the particulate absorption can be considerably more than two orders of magnitude above that due to gases for windy conditions. Fog and battlefield disturbances (including EO countermeasures) also represent a relatively undefined but potentially strongly absorptive environment in terms of particulate absorption.

Since atmospheric aerosols are known frequently to be fragile with respect to composition, e.g., particles with volatile components, it is important to measure their absorption in situ or, in other words, without removing them from their natural environment. Other reasons for the importance of in situ measurements are that neither the bulk properties of many atmospheric particulates nor, on a real-time basis, the chemical composition of these particulates are known.

The spectrophone technique was conceived nearly a century ago by Alexander Graham Bell (5), but applications using laser sources

N-55100 W					
876	<input checked="" type="checkbox"/>	White location			
906	<input type="checkbox"/>	Left location			
WATERPROOF	<input type="checkbox"/>				
CERTIFICATION					
Pex Basic set.					
#1 ASC Vol. I					
CERTIFICATION/INTEGRITY BOOK					
S-2		AVAIL. end/w/ SPENIA			
A					

78 06 12 057

*BRUCE, PINNICK, BREWER, YEE, and FERNANDEZ

(with the advantages of high spectral resolution and power densities) first appeared in 1968 (6); absorption measurements on solids, liquids, and gases have all been reported (7,8). Spectrophones of unique design have been developed in this laboratory for gas and/or aerosol measurements (9). Systems of high sensitivity ($\sim 0.001 \text{ km}^{-1}$) have been developed for measurements with pulsed sources (10) as well as with CW sources (11), with or without windows, and for continuous flow-through operation. Basic to these designs has been an acoustically isolated, resonant inner cavity without windows, which generally operates in a longitudinal acoustical mode in response to the absorption signal. The isolation thereby obtained effectively eliminates the window noise, which has been represented as the perennial spectrophone problem.

A schematic of a microphone is shown in Figure 1. Within this cavity, low-Q longitudinal acoustical modes are established in the gaseous medium from the gaseous or particulate absorption signals.

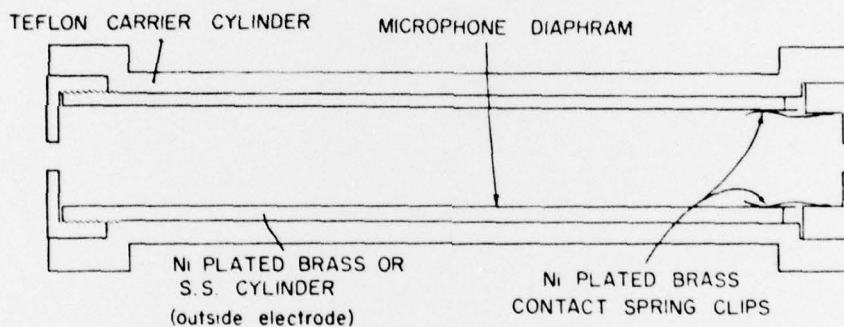


Figure 1. Components of cylindrical microphone.

Spectrophone physical considerations and design parameters have been discussed in a technical report (9); but briefly, the vital points are that the spectrophone system must be designed to produce signals proportional to the absorption coefficient and must be linear with power and be calibratable. Finally, this calibration factor must be independent of the optical wavelength. The accomplishment of these qualities is discussed in the aforementioned report for gaseous absorption, but the same requirements apply to particulate absorption measurements. For the particulates, the above design criteria are manifested in the following concerns: time response of the spectrophone to particulate matter, behavior of volatile components, and variation of the optical constants of the particles as a function of particle temperature. Time response for the particulate material

*BRUCE, PINNICK, BREWER, YEE, and FERNANDEZ

requires a very complicated calculation for precise results but, as simplified somewhat, provides an upper bound for the frequency of the chopped signal. The spectrophone time response can be shown to vary as the square of the particle diameter. The system parameters were designed such that there is no significant net temperature increase in the particle per on-off cycle of the beam. By keeping the maximum particle temperature rise down ($<30\text{ }^{\circ}\text{C}$) the latter two concerns relative to spectrophone design are successfully treated. Temperature rise in the illuminating beam as a function of particle radius was calculated for three of the four substances studied to assure that the design criteria are not violated.

These particle heating results are highly dependent in both spectral form and magnitude on the complex refractive indices. For example, water particle heating is quite constant as a function of radius below about $2\mu\text{m}$, decreasing slowly above that radius, while particle heating for both quartz and ammonium sulfate were peaked with maximum temperatures much higher than for water droplets. The fourth, calcite, was such a weak absorber that in the $9\mu\text{m}$ - $11\mu\text{m}$ region particle heating was not of concern. Though these heating curves were calculated, this type of information may be inferred from the spectrophone results. When absorption is strong, either beam power or beam power density is reduced to reduce heating.

For these absorption measurements, particles which had been ground with mortar and pestle were dispersed in a 0.5 m^3 environmental chamber. Two methods of measurement were used. In one, two CW-source spectrophones were used in a differential mode (12), with one spectrophone continuously sampling air from the chamber and the other sampling ambient air without the particles. Or, if the absorption coefficients of only a few spectral lines were to be measured, a single spectrophone might be used and the ambient values measured prior to and checked following the measurement of dust absorption.

The predominant ambient absorption at the wavelengths of the CO_2 laser used ($9.2\mu\text{m}$ - $10.8\mu\text{m}$) was by water vapor; and, in fact, a strong absorption (at $\text{R}20$, $10.247\mu\text{m}$) was used to calibrate the spectrophone system for both gaseous and particulate absorption measurements. For this purpose dew point sensors are always in operation during absorption measurements.

The measurement procedure for dry particulates was generally to sample the contents of the holding chamber repeatedly with the spectrophone system, with a filter carousel device to collect particles on Nuclepore filters, and with a light-scattering aerosol counter

*BRUCE, PINNICK, BREWER, YEE, and FERNANDEZ

developed by Rosen (13). Scanning electron microscope photomicrographs were subsequently taken of particles collected onto the filters; and these, together with the particle counter results, were used to determine the form of the particle size distribution. The question of the calibration of the particle counter may be found elsewhere (14,15). Here the counter, when operated, was used to obtain only the total concentration of particles with radii $\geq 0.17 \mu\text{m}$.

A schematic of the spectrophone optical path and particle sampling apparatus is shown in Figure 2. The three sampling flow inlets shown, i.e., to the filter carousel, to the particle counter, and to the vertically mounted spectrophone, are in similar proximity and orientation in the actual system. For measurement of the absorption by liquid droplets a larger chamber was constructed ($\sim 1 \text{ m}^3$) and,

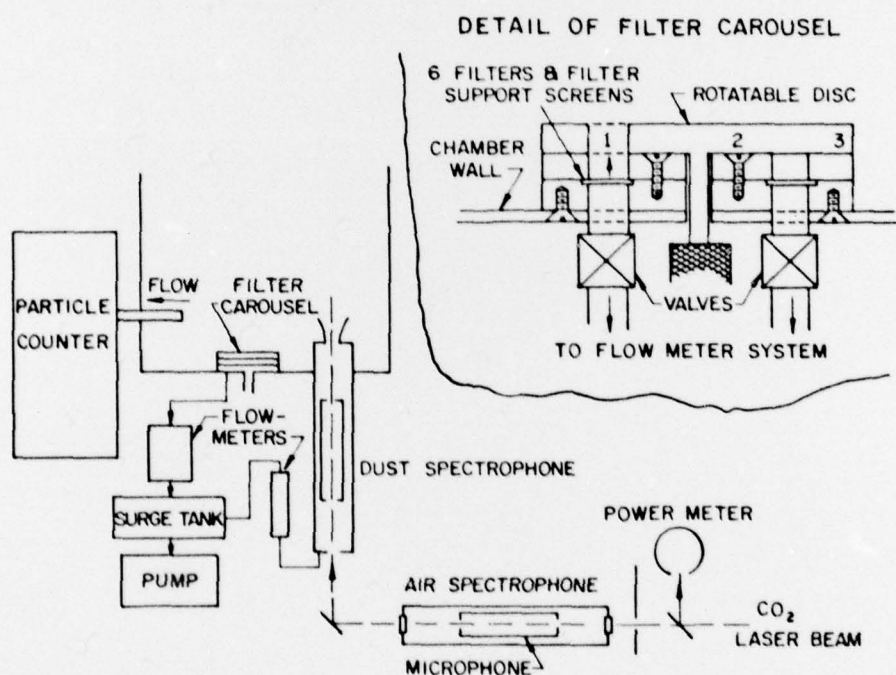


Figure 2. Arrangement of measurement apparatus showing light scattering particle counter, filter particle collectors (6), and spectrophone cutaway. The insert depicts a cross-sectional view of the filter carousel. To obtain a filter sample, the top disk is rotated to expose a filter; and the appropriate valve to the flowmeter is opened.

*BRUCE, PINNICK, BREWER, YEE, and FERNANDEZ

though the spectrophone arrangement is similar to that described for the dry particulates, a commercial "Knollenberg" particle counter is used in place of the Rosen counter and a liquid content measurement takes the place of the filter sample carousel. Intake orifices for each of these plus that of a dew point sensor are in close proximity to each other. The droplets are generated by a commercial mist generator.

Individual droplets cannot be examined in this case but, since they can be assumed to be quite spherical, the particle counter is expected to be relatively accurate since calibration can be performed using spherical particles having various refractive indices (16).

Several particulate substances were selected for absorption studies, the prime consideration being relevance to the atmospheric absorption problem. Absorption studies for particulate quartz, calcite, and ammonium sulfate and preliminary results on liquid water will be presented in this paper.

Quartz was chosen because of the strong spectral dependency of the absorption in the wavelength region for the laser source used, the ready availability of measurements on the bulk properties of the material, and its stable (and minimally hygroscopic) nature, in addition to its frequency of occurrence and relatively strong absorption within the 9 μ m to 11 μ m region.

Measurement of the absorption of dust as a function of settling time in the environmental chamber effectively provides results for a continually changing size distribution. The strong test of correlation between calculated and measured results was an objective of this procedure. Figure 3 shows spectrophone measurements and Lorenz-Mie predictions of the absolute value of the aerosol absorption coefficient (in units of km^{-1}) as a function of time after the quartz samples are dispersed in the holding chamber. To illustrate some of the difficulties and shortcomings of such a comparison, photomicrographs of the quartz particle filter samples are shown in Figure 4. Each of the samples was collected over a 2-min interval at the times t_1 , t_2 , and t_3 identified in Figure 3. The Lorenz-Mie calculations of the particle absorption coefficients were made for polydispersions of quartz spheres of cross-sectional area equivalent to those measured on enlargements of the photomicrographs. The high degree of irregularity of the particles is immediately apparent; thus, the supposition that particles are spherical is not accurate. To further complicate the comparisons, crystalline quartz is birefringent, with distinctly

*BRUCE, PINNICK, BREWER, YEE, and FERNANDEZ

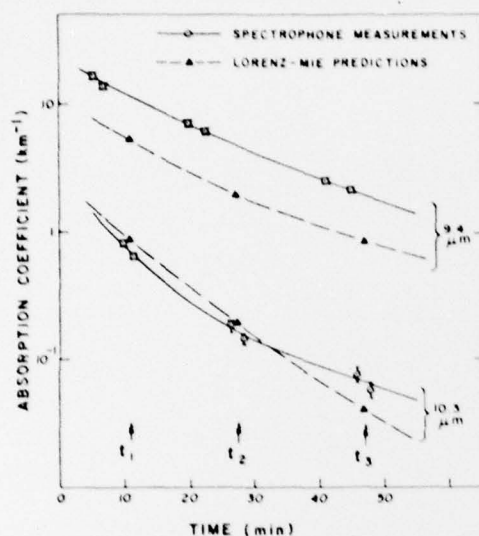


Figure 3. Absorption coefficients of quartz dust as a function of the time after the dust was dispersed in the holding chamber, as predicted by Lorenz-Mie theory and measured with a spectrophone, for two wavelengths. The predictions are based on particle size distributions measured at times t_1 , t_2 , and t_3 .



Figure 4. Scanning electron microscope photomicrographs of quartz particles collected onto Nuclepore filters. The corresponding samples were taken at times t_1 , t_2 , and t_3 (see Fig. 3). Each photograph contains the geometric mean radius r_g and geometric standard deviation σ_g for log normal size distributions obtained by determining the radii of spheres of equivalent cross sections from the SEM photomicrographs. Also shown are the corresponding aerosol mass loadings m , as determined from the log normal size distribution parameters by using a quartz density of 2.6 g cm^{-3} . The dark circles are holes in the Nuclepore filter substrate.

*BRUCE, PINNICK, BREWER, YEE, and FERNANDEZ

different indices of refraction for the ordinary and extraordinary rays. In accordance with the methods of Peterson and Weinman (17), the calculations for the ordinary and extraordinary rays were weighted on a 2:1 basis. These calculations were based on the observed particle size distributions and the complex refractive index for bulk crystalline quartz as reported by Spitzer and Kleinman (18). For the calculational approximations made, the agreement, which is roughly within a factor of 2, should be considered relatively close. It might have been more appropriate to use spheres of equal volume in the calculations of particulate absorption, since the particles were generally small in comparison with the wavelength; however, quantitative estimates of particle volumes from the photomicrographs were not possible.

That the absolute agreement (in magnitude but not in form) of the spectrophone results and the predictions in Figure 3 is better for the $10.3\mu\text{m}$ than for the $9.4\mu\text{m}$ results is probably fortuitous. The measured and predicted time dependencies, however, are quite close for the results at both wavelengths. The slightly different decay times for the two wavelengths are a result of the changing particle size distribution; the agreement between the spectrophone measurements and the predictions of the temporal changes in the particle absorption at both wavelengths is encouraging.

A comparison of spectral dependencies of measured and predicted absorption is shown in Figure 5. The upper three traces are predictions based on samples taken at times t_1 , t_2 , and t_3 , which were previously identified in Figure 3 for different times in the settling process after the ground quartz was dispersed into the holding chamber.

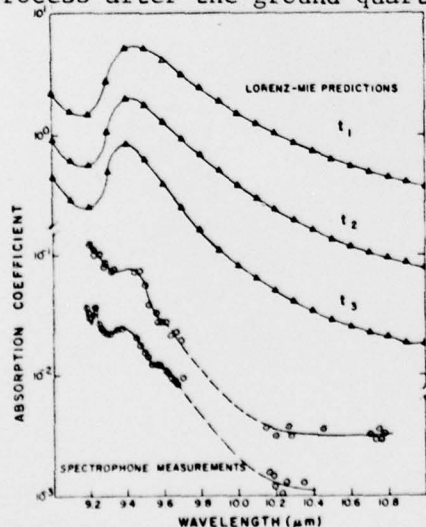


Figure 5. Spectral dependence of the absorption coefficient of quartz dust as predicted from particle size distribution measurements and bulk quartz optical properties by using Lorenz-Mie theory (absolute scale units of km^{-1} , upper three curves) and as measured by using a spectrophone (relative scale, lower two curves). The lower two curves represent data using dust ground from two different bulk quartz samples. The three upper traces correspond to sampling times $t_1 = 11$ min, $t_2 = 27$ min, and $t_3 = 47$ min, as explained in the text.

*BRUCE, PINNICK, BREWER, YEE, and FERNANDEZ

The lowest two traces refer to spectrophone measurements made at times comparable with the approximate time interval from t_2 to t_3 and should, therefore, be compared with the spectral variations shown in the predictions for those times. The spectrophone results represent a number of different measurements that were all normalized to a fixed time. The spectrophone signal time decay was removed by periodically repeating measurement of the absorption signal at particular laser lines. At the longest wavelengths, the absorption fell well below the ambient air absorption (primarily water), and this stressed the subtraction process, though not severely. The resulting errors in measurements of absorption (which are indicated by the spread in the data points) are larger than practical sensitivity limits because, despite the considerable noise in the laboratory during these experiments, no spectrophone acoustic isolation additional to that designed primarily for closed system gaseous absorption measurements was used.

In any case, there is general agreement of the measured and predicted absorption profiles over the $9.2\mu\text{m}$ - $10.8\mu\text{m}$ spectral range, though significantly different behavior is obtained within the $9.2\mu\text{m}$ - $9.4\mu\text{m}$ wavelength region. The upper absorption spectrum shown in Figure 5 for the spectrophone measurements is representative of a number of samples prepared from a block of high purity crystalline quartz. Some significantly different behavior (e.g., a small, sharp peak at $9.22\mu\text{m}$ shown in the lowest curve) has been observed for samples associated with another source of quartz.

Spectrophone measurements of a number of different quartz aerosol samples prepared by the procedures described above showed repeatability of the time and spectral dependencies evident in Figures 3 and 5.

By contrast with quartz the spectral dependence of calcite is very flat and the absorption quite weak in the $9\mu\text{m}$ - $11\mu\text{m}$ wavelength region. Spectrophone measurements of the spectral dependence of calcite agree well with that of spectrophotometer results obtained by the potassium bromide technique. Because of the weak absorption, this common atmospheric ingredient was not studied further.

Ammonium sulfate is also generally believed to be a frequently occurring atmospheric absorber and, like quartz, is known to have a strong absorption between $9\mu\text{m}$ and $10\mu\text{m}$. Once again the measurement process was initiated by grinding and sieving the coarse-grained reagent-grade material and dispersing it within the environmental chamber. The very large particles always settle out quickly and the mean particle radius (and breadth of the size distribution

*BRUCE, PINNICK, BREWER, YEE, and FERNANDEZ

with respect to particle radius) becomes smaller with time, though some deviations from a simple settling process can result due to small amounts of turbulence in the chamber. This can be seen in the sample size distribution data of Figure 6 in which the T-values represent successive times in the settling process. Measurements of the absorption were again compared with results calculated from the particle density as a function of size showing the degree of correlation over a continuously changing distribution. Since ammonium sulfate, like quartz, has a peak absorption at about $9.2\mu\text{m}$ and a relatively weak absorption at $10\mu\text{m}$, lines from each region were used in the spectrophone measurements of absorption as a function of settling time.

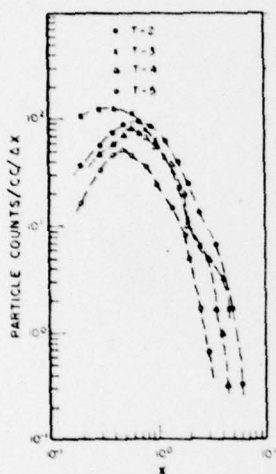


Figure 6. Particle size distribution measurements (shown in units of number/cc/x-interval) vs particle size parameter, $x = 2\pi r/\lambda$. Curves T-2 through T-5 refer to 2-min samples centered at 9.4, 14.4, 20.0, and 33.0 min after dispersal of the dust in the environmental chamber. The first sample, T-1 at 4.2 min showed a heavy concentration of particle clusters and was not analyzed.

Figure 7 shows absorption results for these two frequencies, both as measured and as calculated in the same manner as for quartz. Although ammonium sulfate is trirefringent (quartz was birefringent) the indices do not differ markedly. The size distribution data used in the calculations are shown in the previous figure (6). Here, the $9.25\mu\text{m}$ results are in comparatively close agreement, considering the calculational difficulties, though the time dependencies are different. The $10.22\mu\text{m}$ results for ammonium sulfate show a difference which increases with time--to a point. A consistency which has been noted for the two substances, i.e., quartz and ammonium sulfate, is that the measured spectral dependencies are greater than the calculated quantities and, further, the measured spectral dependence increases with time faster than predicted and then appears to level off. The theory indicates that, for any particulate substance, the spectral dependence becomes independent of particle radius for $r \ll \lambda$. The size distributions of these data approach but do not really satisfy this criterion even at the largest settling time.

*BRUCE, PINNICK, BREWER, YEE, and FERNANDEZ

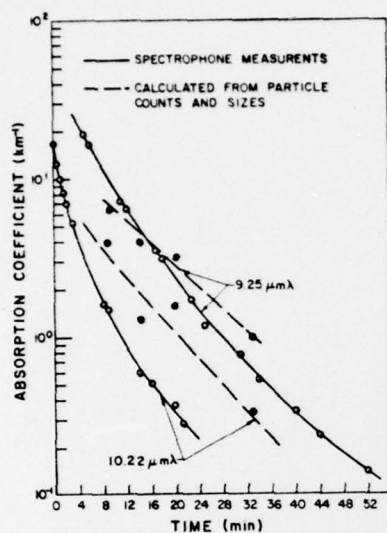


Figure 7. Absorption coefficients of ammonium sulfate dust as a function of time after dispersal, as predicted and measured with a spectrophone, for two wavelengths.

Absorption as a function of particle size parameter is plotted in Figure 8 for $9.25\mu\text{m}$ and $10.22\mu\text{m}$ to show from what size range the significant contributions to the absorption come. For example, at $9.25\mu\text{m}$ approximately 80% of the absorption for the first time period is due to particles between $1.2\mu\text{m}$ and $6.3\mu\text{m}$ and for the last time period particles between $1.0\mu\text{m}$ and $2.9\mu\text{m}$ contribute about the same percentage. Again, at $10.22\mu\text{m}$, 80% of the absorption occurs between $1.2\mu\text{m}$ and $6.3\mu\text{m}$ for the first time period but the radius range is now broader at $1.5\mu\text{m}$ to $3.7\mu\text{m}$ for the last period.

for the first time period but the radius range is now broader at $1.5\mu\text{m}$ to $3.7\mu\text{m}$ for the last period.

It can be seen from Figure 7 that, particularly for the $10.22\mu\text{m}$ calculated absorption, there is considerable fluctuation with settling time. This apparent sensitivity to details of the size distribution and wavelength was not encountered for quartz. Evidence of this sensitivity is also shown in Figure 9.

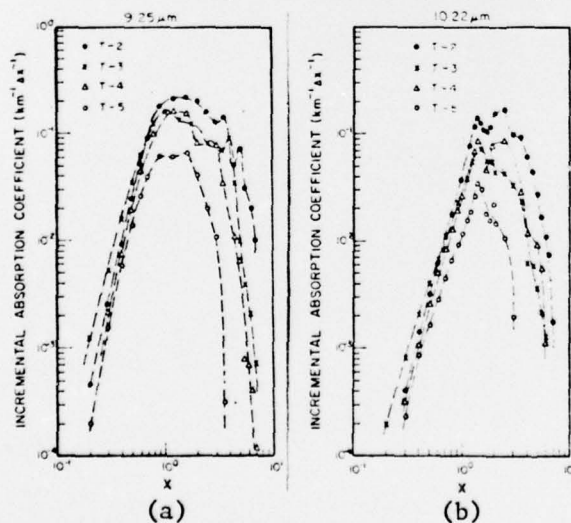


Figure 8. Absorption coefficient per unit size parameter increment as the size parameter for $9.25\mu\text{m}$ (a) and $10.22\mu\text{m}$ (b). Differences in form between the two wavelengths are primarily due to the optical constants.

*BRUCE, PINNICK, BREWER, YEE, and FERNANDEZ

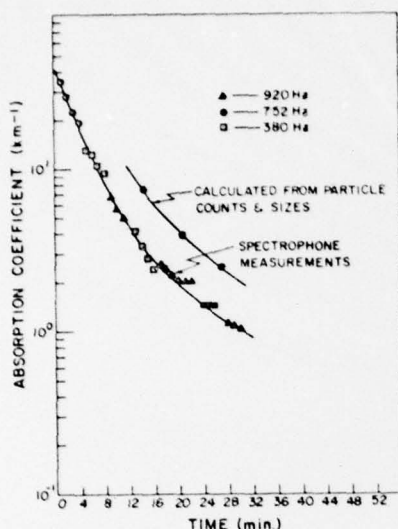


Figure 9. Absorption coefficients of ammonium sulfate dust as a function of settling time after dispersal (similar to Fig. 7) for 9.25 μ m but using three spectrophone chopping frequencies.

This represents another 9.25 μ m series of measurements in the environmental chamber. The spectrophone results are close to those of Figure 7. However, the predicted absorption is now higher though the corresponding "differential" absorption plot does not appear significantly different in form from that of Figure 8.

Another aspect of this particulate data that is of interest relates to the fact that the data were taken for three different chopping rates. The spectrophones were calibrated for each of these rates using the ambient water vapor absorption. Time response calculations indicate that the higher frequencies should be adequate for the particle size distribution encountered, and these data constitute an experimental check on this and should indicate whether the largest particles contributing significantly to the absorption are within the spectrophone response time. The smooth curve shown, in fact, gives no evidence of absorption dependence on the chopping frequencies used.

The overall agreement between spectrophone measurements and calculated values for distributions of particles that are quite irregular, e.g., quartz and ammonium sulfate, is perhaps surprising considering the uncertainty associated with the estimation of the effective cross-sectional areas of the particles. However, measured spectral dependencies do appear to be greater than predicted. The reason(s) for this may be associated with the area estimation just mentioned. If the areas are being overestimated (as is probably the case), the spectral dependence would be reduced. Of course this would also cause a general decrease in magnitude of calculated absorption.

These uncertainties unique to irregular particles should not be of concern in measurement of water droplets found in foggy and hazy environments. The spectral dependence of water absorption in the 9.2 μ m to 10.8 μ m wavelength range is quite flat so the principal question is whether the magnitudes by the two methods agree. The

*BRUCE, PINNICK, BREWER, YEE, and FERNANDEZ

instrumentation, as discussed, gives several points of comparison in close spatial proximity, i.e., the chamber water vapor partial pressure, the total particulate water mass density, the number density as a function of size using a commercial particle spectrometer and the spectrophone spectral absorption values. The water vapor pressure in the chamber was used to calibrate the spectrophone and is the predominant gaseous absorber for the 10 μ m wavelength region--hence dew point and temperature measurements. A measurement of the liquid water content (LWC) was obtained using the particle spectrometer as well as with separate instruments. The check is an important one because of correlations sought between meteorological parameters and absorption values. Though it is not a very stringent test of the particle spectrometer performance, the LWC results have been found to agree very well with the same quantity as measured with the particle spectrometer.

Since water droplets in fogs tend toward large geometric mean radii, spectrophone time response is once again being investigated as a function of chopping frequency for droplet distributions from the largest to be encountered in the chamber to the smallest. Calibration of the particle spectrometer with respect to response as a function of radius and for density is currently uncertain and under investigation.

A number of spectrophone measurements of the water droplet absorption have been made and compared with calculated results based on the particle spectrometer data. These results show agreement within about a factor of two. Comparative results are currently being obtained for a variety of droplet distributions in an attempt to correlate the absorption with simpler measurements in a simple and direct way.

By the time this paper is presented specially designed spectrophone/particle spectrometer systems will have been operated in a field measurement program to identify atmospheric effects on high energy lasers and EO systems at WSMR. The adaptation of the laboratory in situ absorption measurement systems involves a number of design requirements. As an example, low visibility conditions are of prime interest and, for dusty conditions, this frequently implies high wind velocities. The problem arising from this is that the spectrophone must sample the medium without modifying the size distribution or the densities. To cope with the problem, an intake system based on calculations of aero and particle dynamics has been designed to minimize distortion of the atmospheric quantities.

*BRUCE, PINNICK, BREWER, YEE, and FERNANDEZ

Another example is found in the requirement to perform sensitive acoustically based measurements in a high noise level environment. A relatively high degree of acoustical isolation is inherent in the spectrophone design (9), but further acoustic damping for the intake system has been designed and tested. Sample results for spectrophone systems operating between 350 and 750 Hz chopping rates are shown in Figure 10. These mechanical dampers are simply inserted in series with the microphone in the spectrophone system.

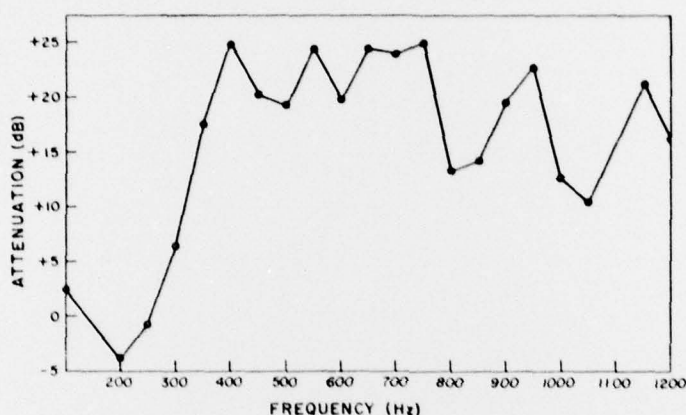


Figure 10. Attenuation of extraneous acoustical noise by spectrophone mechanical filters. Design range from 350 to 750 Hz.

The approach for this measurement program is and has been to study particulate and gaseous absorption under relatively controlled conditions using prototype spectrophone systems and correlative predicted values. On the basis of the experience gained making measurements under laboratory conditions, systems for field measurement programs are then designed, tested and placed in service.

REFERENCES

1. Grams, G. W., I. H. Blifford, Jr., D. A. Gillette, and P. B. Russell, 1974, J. Appl. Meteorol., 13:459.
2. DeLuisi, J. J., P. M. Furukawa, D. A. Gillette, B. G. Schuster, R. J. Charlson, W. M. Porch, R. W. Fegley, B. M. Herman, R. A. Rabinoff, J. T. Twitty, and J. A. Weinman, 1976, J. Appl. Meteorol., 15:455.

*BRUCE, PINNICK, BREWER, YEE, and FERNANDEZ

3. Herman, B. M., R. S. Browning, and J. J. DeLuigi, 1975, J. Atmos. Sci., 32:918.
4. Preliminary results of aerosol absorption measurements (at one wavelength near $10\mu\text{m}$) made using another type of spectrophone and a modified Royco aerosol counter were published by D. Depatie and J. Lentz, 1974, Air Force Weapons Laboratory Laser Digest Report AFWL-TR-74-344, Air Force Weapons Laboratory, Kirtland Air Force Base, New Mexico. These authors hope to complete their analysis and report their results in the open literature.
5. Bell, A. G., 1880, Proc. Am. Assoc. Advancement Sci., 29:115.
6. Kerr, E. L., and J. G. Attwood, 1968, Appl. Opt., 7:915.
7. Rosencwaig A., 1973, Science, 181:657.
8. Harshbarger, W. R., and M. B. Robin, 1973, Acc. Chem. Res., 6:329.
9. Bruce, C. W., 1976, "Development of Spectrophones for CW and Pulsed Radiation Sources," R&D Report, ECOM-5802, Atmospheric Sciences Laboratory, US Army Electronics Command, White Sands Missile Range, New Mexico.
10. Bruce, C. W., B. Z. Sojka, B. G. Hurd, R. Watkins, K. O. White, and Z. Derzko, 1976, Appl. Opt., 15:2970.
11. Bruce, C. W., 1975, J. Opt. Soc. Am., 65:1163A.
12. Bruce, C. W., 1976, J. Opt. Soc. Am., 66:1071A.
13. Rosen, J. M., 1964, J. Geophys. Res., 64:4673.
14. Pinnick, R. G., J. M. Rosen, and D. J. Hofmann, 1973, Appl. Opt., 12:37.
15. Pinnick, R. G., and D. J. Hofmann, 1973, Appl. Opt., 12:2593.
16. Pinnick, R. G., "Response Characteristics of Knollenberg Light Scattering Aerosol Counters" (to be published).
17. Peterson, J. T., and J. A. Weinman, 1969, J. Geophys. Res., 74:6497.
18. Spitzer, W. G., and D. A. Kleinman, 1961, Phys. Rev., 121:1324.